



# UserCalc: A Web-based uranium series calculator for magma migration problems

M. Spiegelman

Lamont-Doherty Earth Observatory of Columbia University, Palisades, New York 10964  
(mspieg@ldeo.columbia.edu)

[1] **Abstract:** Measured departures from secular equilibrium in the uranium series decay chains provide important constraints on the rates of recent mantle and crustal processes. Nevertheless, the inferences drawn from these observations depend upon the models used to interpret them. While several useful models for U series exist, they are not all equally easy to use, and it is often the ease of use, rather than the utility of the model, that determines which models are applied. The purpose of this paper is to level the playing field by making some of the more general U series transport models accessible to a wider community through the UserCalc Web site available from Lamont-Doherty Earth Observatory at [www.ldeo.columbia.edu/~mspieg/UserCalc/](http://www.ldeo.columbia.edu/~mspieg/UserCalc/). These models calculate the effects of both melting and melt transport on two U series chains ( $^{238}\text{U} \rightarrow ^{230}\text{Th} \rightarrow ^{226}\text{Ra}$  and  $^{235}\text{U} \rightarrow ^{231}\text{Pa}$ ) and allow the user to input their own petrological insight and data to explore the behavior of this model. The purpose of the site is to provide a tool that can spur additional collaborations between geophysicists and geochemists as well as drive more rapid exploration/evolution of U series models.

**Keywords:** Uranium series disequilibrium; geochemical models; mantle modeling; magma dynamics; mid-ocean ridges; island arcs.

**Index Terms:** Magma migration; geochemistry; modeling; numerical solutions.

**Received** November 11, 1999; **Revised** June 19, 2000; **Accepted** July 7, 2000; **Published** August 11, 2000.

Spiegelman, M., 2000. UserCalc: A Web-based uranium series calculator for magma migration problems, *Geochem. Geophys. Geosyst.*, vol. 1, Paper number 1999GC000030 [4482 words, 3 figures]. Published August 11, 2000.

## 1. Introduction

[2] Radioactive decay chains such as the two uranium series  $^{238}\text{U} \rightarrow ^{230}\text{Th} \rightarrow ^{226}\text{Ra}$  and  $^{235}\text{U} \rightarrow ^{231}\text{Pa}$  are unique among commonly measured geochemical tracers in their ability to place constraints on the rates of recent mantle processes. Because the longer-lived daughter nuclides in this series have half-lives ranging from 1600 to 245,500 years, they are

particularly sensitive to processes such as the rate of mantle melting or the flow rates of convection or melt transport. In conjunction with stable trace elements, major elements, and long-lived isotopic systems (e.g., Sm/Nd, Rb/Sr, ...) the U series nuclides provide important complementary information for inferring the properties and processes occurring in the Earth's mantle. Nevertheless, like most proxy measurements, the actual inferences

drawn from the observations depend significantly on the models used to interpret them.

[3] For the U series, there are several standard models available for modeling the observed departures from secular equilibrium due to mantle melting. The simplest models are batch-melting models [e.g., *Allègre and Condomines*, 1982; *Sims et al.*, 1995], which assume that the maximum variations from secular equilibrium are due solely to chemical fractionation. These models may work for very small degrees of melting (e.g., beneath ocean islands [*Sims et al.*, 1995, 1999]) but are problematic for degrees of melting  $F$  much larger than the partition coefficients of the U series nuclides ( $D \approx 0.001$ ) because solutions with  $F \gg D$  produce negligible chemical fractionation. More complex “dynamic melting” ingrowth models [e.g., *McKenzie*, 1985; *Williams and Gill*, 1989; *Qin*, 1992; *Richardson and McKenzie*, 1994; *Iwamori*, 1994] assume slow, near-fractional melting and instantaneous melt extraction. These models produce excess daughter products by increasing the residence time in the solid of the parent relative to the daughter during melting. These models place constraints on melt generation rates and the volume of equilibration but not on the actual melt transport process because they do not include the mechanics of melt transport. The most general U series models to date [*Spiegelman and Elliott*, 1993; see also *Lundstrom et al.*, 1995; *Iwamori*, 1994], however, include the coupled processes of adiabatic melting and melt extraction and calculate the consequences of both processes for U series excesses.

[4] All of these models are useful; however, they are not all equally easy to use. Both batch-melting and the simplest dynamic melting models have analytic solutions and are easily calculated on a spreadsheet. The transport models, however, require accurate nu-

merical integration of ordinary differential equations (ODEs). Good ODE integrators can be found in many packages but require a bit more work to implement. Unfortunately, the extra effort required to implement these models is usually sufficient to deter all but the most eager investigators, with the result that potentially useful models do not get used. This is a disservice to users of models because it limits the tools that are available to them, and it is also a disservice to the modeler because it limits the population of people who can test and evaluate the worth of the model. Fortunately, given modern distributed computing, platform-independent user interfaces (e.g., the Web), and electronic publications such as *Geochemistry, Geophysics, Geosystems (G<sup>3</sup>)*, it is now relatively straightforward for modelers to make their models accessible and available to the entire community. The purpose of this paper and Web site (available from Lamont-Doherty Earth Observatory at <http://www.ldeo.columbia.edu/~mspieg/UserCalc>) is to implement this approach to community models in solid Earth science by making available an extended model for U series in mantle melting based on the models of *Spiegelman and Elliott* [1993]. The hope is that improved access will increase the body of users of the model, begin a better dialog between producers and users of models, and lead to a better integration of theory and observation. If this exercise proves useful, additional models can readily be added to the site. The remainder of this paper will describe the underlying mechanics of the model and its implementation through the UserCalc Web site.

## 2. The Model

[5] The basic model is an extension of the equilibrium transport model of *Spiegelman and Elliott* [1993], and the derivation follows from that paper. As implemented here, the model

calculates the concentrations and activities of the two U series chains  $^{238}\text{U} \rightarrow ^{230}\text{Th} \rightarrow ^{226}\text{Ra}$  and  $^{235}\text{U} \rightarrow ^{231}\text{Pa}$  for a one-dimensional (1-D) upwelling column undergoing melting by adiabatic decompression. Melt extraction is governed by a simplified form of Darcy's law, and the melt is assumed to remain in chemical equilibrium with the solid matrix during transport (although this is readily modified in other versions of the code). The model begins with conservation of mass for the melt, solid, and each component in the decay chain. For a 1-D steady state model these can be written as

$$\frac{\partial}{\partial z} \rho_f \phi w = \Gamma, \quad (1)$$

$$\frac{\partial}{\partial z} \rho_s (1 - \phi) W = -\Gamma, \quad (2)$$

$$\begin{aligned} \frac{\partial}{\partial z} [(\rho_f \phi w + \rho_s (1 - \phi) W D_i) c_i^f] \\ = \lambda_{i-1} \bar{\rho} \bar{D}_{i-1} c_{i-1}^f - \lambda_i \bar{\rho} \bar{D}_i c_i^f, \end{aligned} \quad (3)$$

where  $\rho_f$  and  $\rho_s$  are melt and solid densities,  $w$  and  $W$  are melt and solid velocities,  $\phi$  is the porosity, and  $\Gamma$  is the "melting rate" or rate of mass transfer from solid to liquid. In (3),  $D_i$  is the bulk partition coefficient of element  $i$  in each chain, and  $c_i^f$  is the concentration of that element in the melt. The local solid concentration is therefore  $c_i^s = D_i c_i^f$ . Here  $\lambda_i$  is the decay constant for element  $i$ , and

$$\bar{\rho} \bar{D}_i = \rho_f \phi + \rho_s (1 - \phi) D_i \quad (4)$$

such that  $\bar{\rho} \bar{D}_i c_i^f$  is the total mass per unit volume of component  $i$  in the melt plus solid. All variables subscripted  $i-1$  imply the parent element up the chain. For elements with no parents (i.e.,  $^{238}\text{U}$  and  $^{235}\text{U}$ ),  $\lambda_{i-1} = 0$ .

[6] For this model, the melting rate  $\Gamma$  is chosen for a 1-D adiabatic melting column such that

$$\Gamma = \rho_s W_0 \frac{\partial F}{\partial z}, \quad (5)$$

where  $W_0$  is the solid upwelling velocity at the base of the melting column ( $z = 0$ ) and  $F$  is the

degree of melting and is a function of height in the melting column and is a function of height in the melting column.

[7] Equations (1)–(2) (and (5)) govern the total conservation of mass for melt and solid phases while (3) governs conservation of mass for each component  $i$  in the bulk equilibrium system of melt plus solid. Equation (3) allows for both radioactive production and decay. Given just conservation of mass and composition, (1)–(5) can be rewritten into a system of ordinary differential equations for the concentration of each nuclide in the melt. The basic derivation is given by *Spiegelman and Elliott* [1993] with the result

$$\begin{aligned} \frac{dc_i^f}{dz} = \frac{-c_i^f}{F + (1 - F)D_i} \frac{d}{dz} [F + (1 - F)D_i] \\ + \frac{[\lambda_{i-1} \bar{\rho} \bar{D}_{i-1} c_{i-1}^f - \lambda_i \bar{\rho} \bar{D}_i c_i^f]}{\rho_s W_0 [F + (1 - F)D_i]}, \end{aligned} \quad (6)$$

where now both  $D_i$  and  $F$  are allowed to be variable functions of height  $z$ . Equation (6) governs changes in concentration of element  $i$  in the melt with height and has two terms. The first term governs changes in concentration due to melting and changes in partition coefficient. This term is identical to that expected for true batch melting and is independent of porosity and upwelling rate [see *Ribe, 1985; Spiegelman and Elliott, 1993*]. The second term, however, is the "ingrowth" term, which controls changes in concentration due to the balance of radioactive production and decay. This term is sensitive to both  $\phi$  and  $W_0$  as these affect the relative residence times of parent and daughter elements in the melting column.

[8] Equation (6) is actually solved in a more numerically tractable form by defining

$$U_i^f = \ln \frac{c_i^f}{c_{i0}^f}, \quad (7)$$

where  $c_{i0}^f = c_{i0}^s / D_i^0$  is the concentration of the first instantaneous melt at the base of the

melting column. Here  $c_{i0}^s$  is the concentration of element  $i$  in the unmelted solid, and  $D_i^0$  is the partition coefficient at  $z = 0$ . Noting that

$$\frac{dU_i^f}{dz} = \frac{1}{c_i^f} \frac{dc_i^f}{dz}, \quad (8)$$

(6) can be divided by  $c_i^f$  and rewritten as

$$\frac{dU_i^f}{dz} = \frac{-1}{F + (1-F)D_i} \frac{d}{dz} [F + (1-F)D_i] + \frac{\lambda_i}{w_{\text{eff}}^i} [R_i^{i-1} \exp[U_{i-1}^f - U_i^f] - 1] \quad (9)$$

where

$$w_{\text{eff}}^i = \frac{\rho_f \phi w + \rho_s (1 - \phi) D_i W}{\rho_f \phi + \rho_s (1 - \phi) D_i} \quad (10)$$

is the “effective velocity” of element  $i$  which varies from  $w$  when  $D_i = 0$  to  $W$  when  $D_i \rightarrow \infty$ . The effective velocity can also be rewritten using (1), (2), and (5) as

$$w_{\text{eff}}^i = \frac{\rho_s W_0 [F + (1-F)D_i]}{\rho_f \phi + \rho_s (1 - \phi) D_i}. \quad (11)$$

Finally,

$$R_i^{i-1} = \alpha_i \frac{D_i^0}{D_{(i-1)}^0} \frac{\rho D_{i-1}}{\rho D_i} \quad (12)$$

is the ingrowth factor for elements  $i-1$  and  $i$ . Here  $\alpha_i = (\lambda_{i-1} c_{(i-1)0}^s / \lambda_i c_{i0}^s)$  is the activity ratio of parent to daughter elements in the initial unmelted solid. *Spiegelman and Elliott [1993]* assumed that all elements were in secular equilibrium before melting (i.e.,  $\alpha_i = 1$  for all elements). The latest version of UserCalc, however, allows for more general initial conditions. This has been prompted by work in subduction zones where it is likely that large influxes of uranium have been added from the slab before significant wedge melting begins [e.g., *Newman et al., 1984; Gill and Williams, 1990; McDermott and Hawkesworth, 1991; Elliott et al., 1997*].

[9] Given  $F(z)$  and  $D_i(z)$  as input, we only need to specify the porosity  $\phi(z)$  to close (9). For a 1-

D steady state column, (1) and (5) can be integrated with boundary conditions  $\phi(0) = F(0) = 0$  to show that

$$\frac{w}{W_0} = \frac{\rho_s F}{\rho_f \phi} \quad (13)$$

so that the melt velocity relative to the solid upwelling velocity is controlled by the ratio of degree of melting to the porosity. Thus any  $\phi(z) \leq \rho_s F(z) / \rho_f$  is a valid solution and could be imposed entirely in an ad hoc manner. However, it is somewhat more physical to have the melt flow and porosity be governed by a simplified version of Darcy’s law for a permeable medium

$$\phi(w - W) = k_\phi \Delta \rho g (1 - \phi), \quad (14)$$

where

$$k_\phi = k(z) \phi^n \quad (15)$$

is the permeability that is assumed to be a power law in porosity with a spatially varying prefactor  $k(z)$ ;  $\Delta \rho g$  is the buoyancy difference between solid and melt. ( $\Delta \rho = \rho_s - \rho_f$ , and  $g$  is the acceleration due to gravity). Integrating (1), (2), and (5) with boundary conditions  $\phi(0) = F(0) = 0$  and  $W(0) = W_0$  and substituting into (14) yield an implicit polynomial relationship for  $\phi(z)$ .

$$\left[ \frac{\rho_s F}{\rho_f} - \frac{\phi(1-F)}{(1-\phi)} \right] = A(z) \phi^n (1-\phi), \quad (16)$$

where

$$A(z) = k(z) \frac{\Delta \rho g}{W_0}. \quad (17)$$

If  $k(z)$  were known, (16) could be solved (numerically) for  $\phi$  immediately; however, as permeability is usually not well known, it is more convenient to calibrate  $A$  by setting the porosity at the top of the column ( $z = d$ ) to some reference porosity  $\phi_0$ , which fixes  $A$  at  $z = d$  to

$$A_d = \left[ \frac{\rho_s F_{\text{max}}}{\rho_f} - \frac{\phi_0(1-F_{\text{max}})}{(1-\phi_0)} \right] / \phi_0^n (1-\phi_0), \quad (18)$$

where  $F_{\max}$  is the porosity at the top of the melting column. We can then define the “relative permeability function” as

$$k_r(z) = k(z)/k(d), \quad (19)$$

which gives the spatially varying component of permeability relative to its value at  $z = d$  (All the solutions in *Spiegelman and Elliott* [1993] assume that  $k_r = 1$  everywhere). With these definitions the polynomial for  $\phi(z)$  that is zero at  $z = 0$  and  $\phi_0$  at  $z = d$  and satisfies both mass conservation and Darcy’s law is

$$k_r(z)A_d\phi^n(1 - \phi)^2 + \phi \left[ 1 + F \left( \frac{\rho_s}{\rho_f} - 1 \right) \right] - \frac{\rho_s}{\rho_f} F = 0. \quad (20)$$

For highly permeable systems (large  $A_d$  and  $\phi \ll F \ll 1$ ) the porosity is approximately

$$\phi(z) \approx \left[ \frac{\rho_s F}{\rho_f k_r A_d} \right]^{1/n}. \quad (21)$$

Given  $\phi_0$ ,  $W_0$ ,  $F(z)$ , and  $k_r(z)$ , the porosity  $\phi(z)$  is determined everywhere in the melting column.

### 3. Implementation

[10] Equations (9) and (20) form a closed system of ordinary differential equations that can be solved for any number of decay chains within the same physical system. These equations are solved numerically using a fifth-order Runge-Kutte Cash-Carp ODE solver with adaptive stepping. A Brent algorithm is used to find roots of (20) (for both, see *Press et al.* [1992]). Initial conditions are  $U_i^f = 0$  for all elements, and there is a single input tolerance (default  $10^{-6}$ ), which controls the relative accuracy of the ODE solvers. These routines are implemented in an optimized Fortran program. The UserCalc Web site forms a wrapper for controlling the input of this program as well as providing graphical and textual output.

[11] As implemented, UserCalc solves for the concentrations and activity ratios of the two decay chains  $^{238}\text{U} \rightarrow ^{230}\text{Th} \rightarrow ^{226}\text{Ra}$  and  $^{235}\text{U} \rightarrow ^{231}\text{Pa}$  given  $W_0$  (in cm/yr),  $\phi_0$ , permeability exponent  $n$ , and initial relative activities  $a_i$  for each element. (The model only requires the initial activity ratios  $\alpha_i = a_{i-1}/a_i$ , but it is easier to input individual activities and then calculate their ratios.) In addition, the model requires input for the continuous functions  $F(z)$ ,  $k_r(z)$ , and  $D_i(z)$ , which are input in tabular form as a spreadsheet and then interpolated using cubic splines. Since it is more common in petrology to give melting functions in terms of pressure, the actual spreadsheet is a seven-column, tab- (or space-) separated spreadsheet with the following columns:  $P$  (kbar),  $F(P)$ ,  $k_r(P)$ ,  $D_{\text{U}}$ ,  $D_{\text{Th}}$ ,  $D_{\text{Ra}}$ , and  $D_{\text{Pa}}$ , where the pressure  $P$  is converted to depth by inputting a single constant pressure gradient  $\partial P/\partial z$  in kbar/km.

[12] This spreadsheet can be calculated in any manner the user chooses and simply passed to the Web site. However, as the spline routines will produce artifacts around steps or sharp changes in properties, one should make sure that there is sufficient resolution around such features. For convenience, UserCalc provides a spreadsheet calculator to provide spreadsheets in the proper format for a simple two-layer model (see Figure 1). In this model (which might be appropriate for melting columns that span the garnet-spinel transition) the lower layer extends from  $P_{\max}$  to  $P_1$ , and  $F(P)$  increases linearly from zero to  $F_1$ . The upper layer extends from pressure  $P_1$  to  $P_{\min}$ , and  $F(P)$  increases linearly from  $F_1$  to  $F_{\max}$ . Each layer can have a different partition coefficient for each element, and the lower layer can have a different intrinsic relative permeability  $k_r$  than the upper layer (which has  $k_r = 1$  by definition).

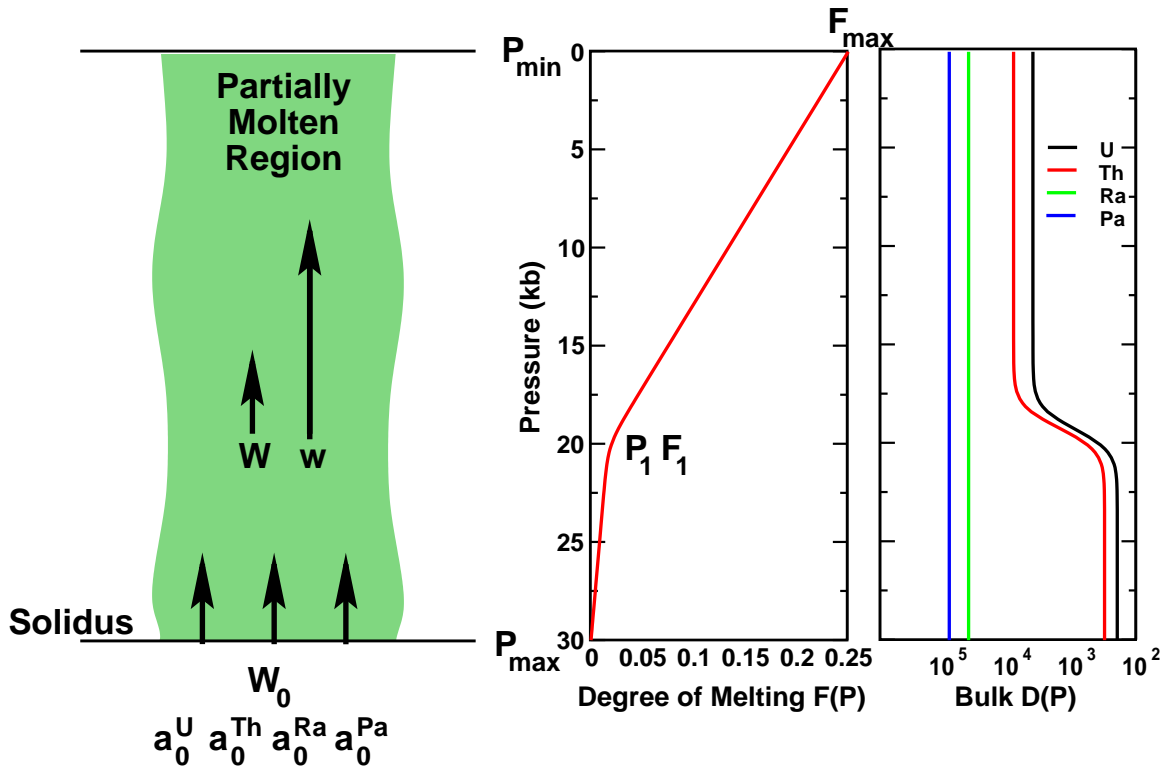


**Figure 1.** General model inputs including  $F(P)$  and  $D_i(P)$  from the two-layer model spreadsheet calculator.

[13] With these inputs, the Web site implements the intrinsic model in two formats: a single 1-D column model showing the changes with height and as contour plots showing the pattern of activity ratios at the top of a set of columns that use the same spreadsheet but span a two-dimensional parameter space in upwelling rate  $W_0$  and maximum porosity  $\phi_0$ . The best approach is probably just to go to the Web site and start playing (all forms have reasonable default values to start). If you prefer to read the manual, however, each module is described here in more detail.

### 3.1. Column Models

[14] The direct output of the column model is a comma-separated spreadsheet with columns pressure (kbar), depth (km),  $F$  |  $\phi$ , ( $^{230}\text{Th}/^{238}\text{U}$ )

( $^{226}\text{Ra}/^{230}\text{Th}$ ) ( $^{231}\text{Pa}/^{235}\text{U}$ ),  $U_{238\text{U}}^f$ ,  $U_{230\text{Th}}^f$ ,  $U_{226\text{Ra}}^f$ ,  $U_{235\text{U}}^f$  |  $U_{231\text{Pa}}^f$  |  $D_U$  |  $D_{\text{Th}}$  |  $D_{\text{Ra}}$  |  $D_{\text{Pa}}$ , and  $z'$ , where  $z'$  is the dimensionless height of the column ( $0 \leq z' \leq 1$ ). The output form also provides tables showing activity ratios at the top of the column, the ratio of melt velocity to solid velocity ( $w_0/W_0$ ) at the top of the column, and some other information about the run (there is also a glossary of terms on the site to explain specific items).

[15] In addition to numeric output, however, the site also provides graphics. Figure 2 shows some of the graphical output of the 1-D column models that compares the vertical structure of the porosity  $\phi$  to the degree of melting  $F$ , the partition coefficient structure with height, and the activity ratios for the three daughter-parent



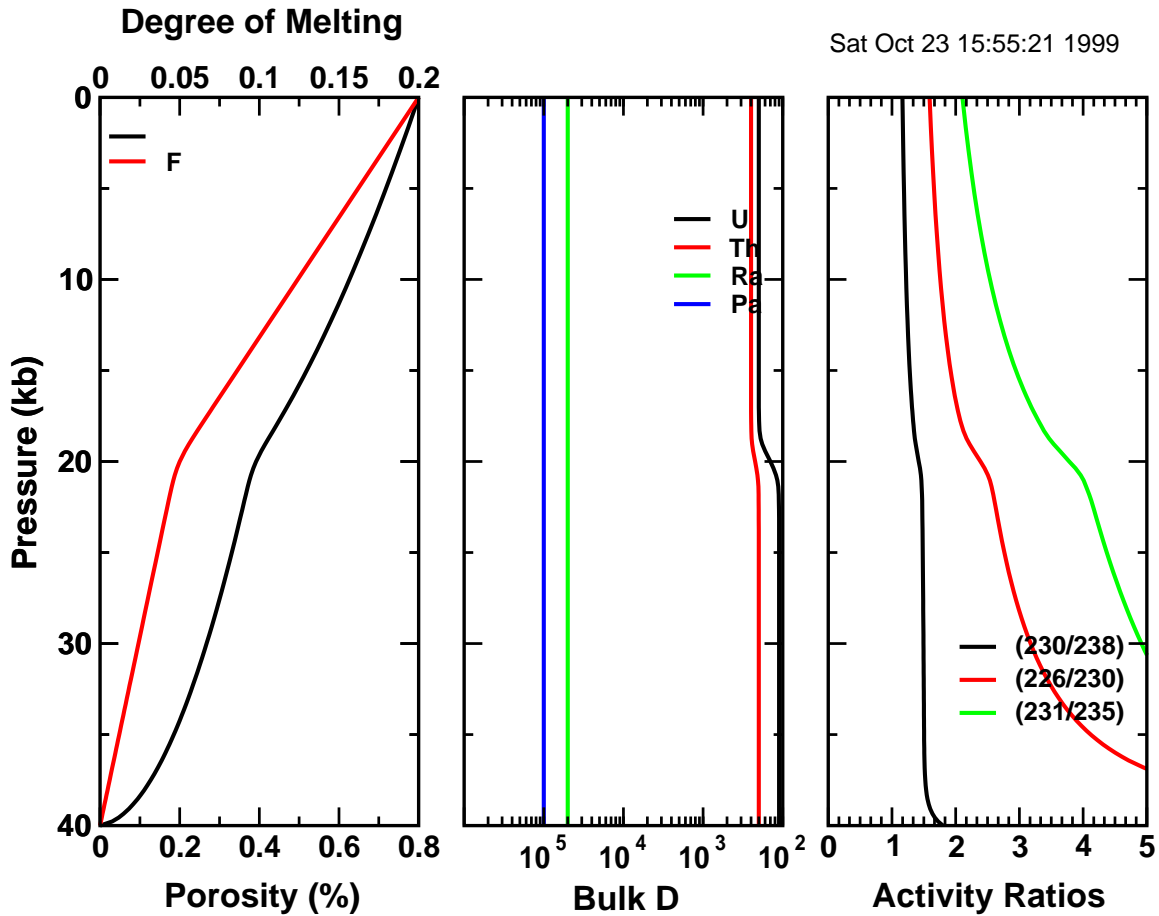


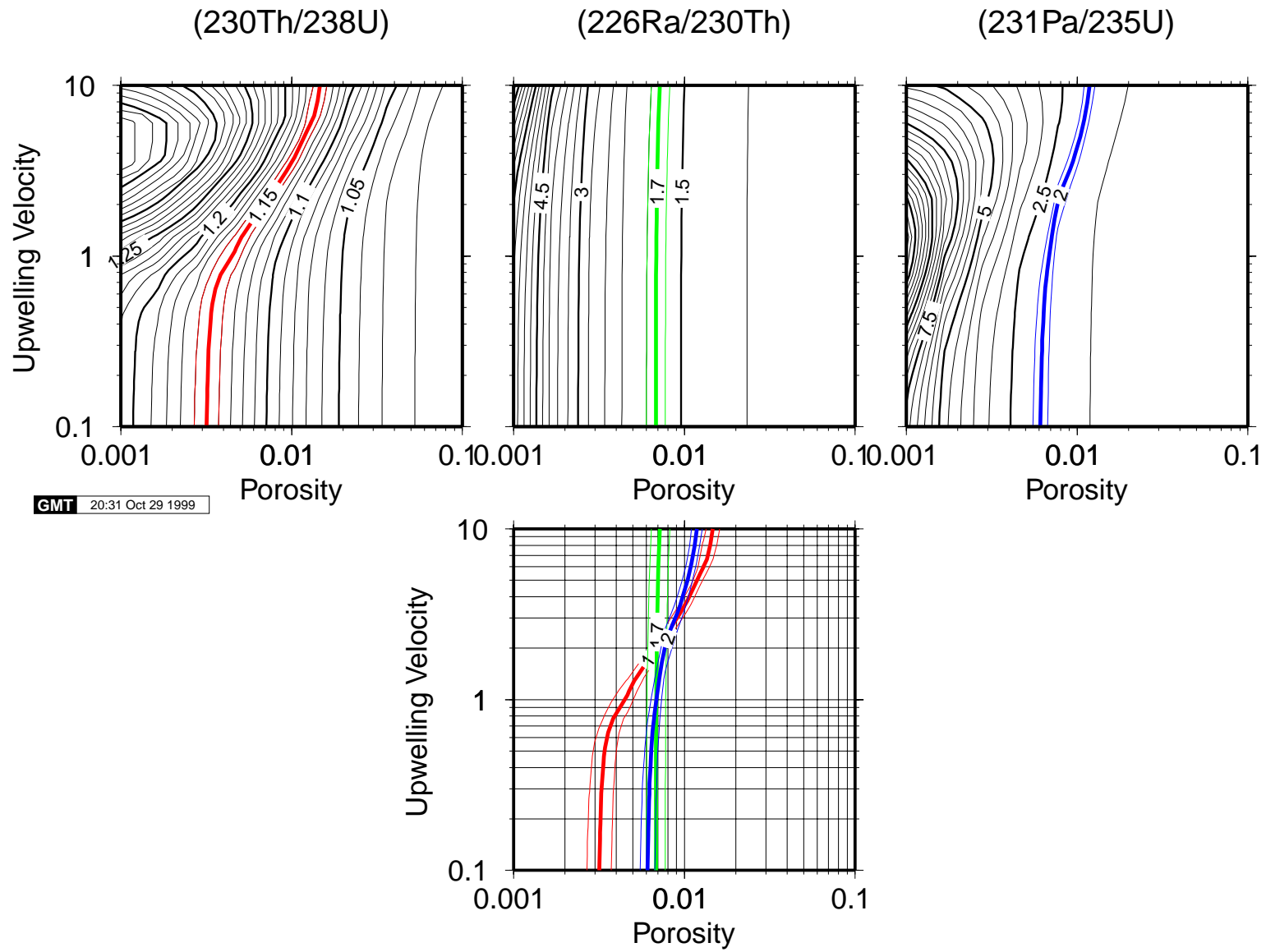
**Figure 2.** Example graphical output of the 1-D column models. The left plot shows porosity  $\phi$  and degree of melting  $F$  as a function of pressure (note the two different horizontal scales for  $\phi$  and  $F$ ; in general,  $\phi \ll F$ ). The middle plot shows bulk partition coefficients as a function of pressure  $D(P)$  (which are different from those in Figure 1). The right plot shows calculated activity ratios versus pressure for the three principal daughter-parent pairs. All of these data (and more) are also provided numerically as a comma-separated spreadsheet.

pairs ( $^{230}\text{Th}/^{238}\text{U}$ ), ( $^{226}\text{Ra}/^{230}\text{Th}$ ), and ( $^{231}\text{Pa}/^{235}\text{U}$ ). This graphical output is supplied as gif images and as either encapsulated postscript files (eps) or pdf files, depending on user choice.

### 3.2. Contour Plots

[16] The 1-D column models are useful for understanding the effects of the input parameters on the vertical structure of concentration

and porosity within the melting column. However, it can be tedious to use this version of the model to explore parameter space. For this reason, the second implementation of the model is in the form of contour plots which allow exploration over a 2-D parameter space of porosity and upwelling velocity. The spreadsheet and other input variables are identical to the 1-D column models; this module simply runs a series of 1-D columns over a 2-D parameter space of  $W_{\min} \leq W_0 \leq W_{\max}$  and





$\phi_{\min} \leq \phi_0 \leq \phi_{\max}$ . The parameter space is sampled logarithmically at  $m \times n$  points ( $m$  and  $n$  can be chosen each to vary from 3 to 30 points in each dimension). The output in these models is a 2-D grid of concentrations and activity ratios at the top of the columns. Numerical output can be requested in ASCII, GMT (.grd), or matlab (.mat) formats and will be returned as a compressed tar file. Graphical output is contour plots of activity ratios as a function of porosity and upwelling rate for the three daughter-parent pairs ( $^{230}\text{Th}/^{238}\text{U}$ ), ( $^{226}\text{Ra}/^{230}\text{Th}$ ), and ( $^{231}\text{Pa}/^{235}\text{U}$ ) and is provided as gif files and EPS or PDF files. Figure 3 shows some of the contour plots. Given a solution, additional replotting of contours and annotation is available.

[17] In addition to simply contouring the output of the model, this module also includes the ability to overlay target data onto the solutions to compare data to models. This target data could be actual measurements from single analyses or composite ranges of activity ratios for a region. The site does not know or care; you just put in three target values for ( $^{230}\text{Th}/^{238}\text{U}$ ), ( $^{226}\text{Ra}/^{230}\text{Th}$ ), and ( $^{231}\text{Pa}/^{235}\text{U}$ ) and an optional set of range parameters  $\sigma_i$ . If this feature is selected, three extra contours ( $\alpha_i - \sigma_i$ ,  $\alpha_i$ , and  $\alpha_i + \sigma_i$ ) are added to each contour plot (see Figure 3). In addition, a fourth plot superposes the three target contours on the same  $\phi_0, W_0$  diagram for direct comparison. Valid solutions of the model that are consistent with the data occur in regions where the three contours intersect. The potentially strong constraints from coupled U series models arise

from the significantly different structures of contours for different nuclide pairs. The behavior of the contour plots and their relationship to the underlying physical parameters are discussed in detail by *Spiegelman and Elliott* [1993]. The principal results, however, are that  $^{230}\text{Th}$  has a long enough half-life such that excesses produced in the bottom of the column can be preserved at the surface if mantle upwelling is sufficiently rapid. In this regime the activity ratio ( $^{230}\text{Th}/^{238}\text{U}$ ) is most sensitive to the upwelling rate  $W_0$ . Very short-lived nuclides such as  $^{225}\text{Ra}$ , however, only see the top of the column and are principally sensitive to the porosity  $\phi_0$ , so that these contours can readily intersect the ( $^{230}\text{Th}/^{238}\text{U}$ ) contours. However,  $^{231}\text{Pa}$ , with its intermediate half-life but very small partition coefficient, behaves somewhere between Th and Ra. Finding intersections of all three systems can be challenging (and is left as an exercise for the reader).

#### 4. Discussion

[18] The principal purpose of this contribution is to begin exploring a new mode of model accessibility for which  $G^3$  is ideally suited. The models in the UserCalc Web site are extended from those of *Spiegelman and Elliott* [1993] but are not radically new. What is new is their accessibility and distribution to a much larger audience of potential users. The benefits of wider accessibility should be apparent. First, this Web site provides a relatively flexible framework for both geophysicists and geochemists to explore the quantitative (and potentially observable) consequences of their own

---

**Figure 3.** Two-dimensional contour plot output. The black lines in the top three plots show contours of activity ratios calculated for the three daughter-parent pairs ( $^{230}\text{Th}/^{238}\text{U}$ ), ( $^{226}\text{Ra}/^{230}\text{Th}$ ), and ( $^{231}\text{Pa}/^{235}\text{U}$ ), plotted in  $\log \phi_0, \log W_0$  space. These plots contour the results of  $10 \times 10$  1-D columns distributed evenly across the 2-D parameter space  $\log \phi, \log W_0$ . In addition, colored contours are shown for the three target values ( $^{230}\text{Th}/^{238}\text{U} = 1.15 \pm 0.01$ , ( $^{226}\text{Ra}/^{230}\text{Th} = 1.7 \pm 0.1$ , and ( $^{231}\text{Pa}/^{235}\text{U} = 2 \pm 0.1$ ). The bottom plot superposes the three target data contours on a single  $\phi_0, W_0$  diagram. Valid model solutions that are consistent with the target data occur where all three contours interact.

ideas about mantle melting on U series. In particular, the new models provide significant latitude to vary parameters such as partition coefficients and permeabilities. By increasing the number of users this approach allows parallel exploration of parameter space driven by real data and scientific agendas beyond that of the model provider. This, in turn, should provide more efficient verification/rejection of these models. Finally, by providing a common platform for spurring collaboration and discussion this approach could lead to a more efficient evolution and extension of these sorts of models driven by an appropriate balance of community interest, data, and the current state of the art in modeling.

[19] The potential benefits of this approach are clear, as are the obvious pitfalls. Recognizing the difference between private “research” code and robust “public” code, the immediate danger of releasing useful but (possibly) buggy code to the public is that I could easily spend significant time tweaking and fixing the site at the expense of other science. More interesting but equally serious is that if the site is actually useful, I could also spend significant time helping users to understand the output of the models and the inferences that could/should be drawn from them. In general, this is good, as the principal purpose of the site is to build interesting scientific collaborations. Nevertheless, there is an unstated issue of etiquette that comes with giving away any intellectual product. To clarify matters, I have put a statement of usage etiquette for the UserCalc Web site up on the introductory page of that site.

[20] The previous pitfalls are readily addressed by common courtesy. The final danger in making models easy to use is their indiscriminate use as “black boxes.” The field is littered with problems where important data have been interpreted with useful but inappropriate models (Lord Kelvin and the age of the Earth

comes to mind), and I have no doubt that the same will be true of these models. Nevertheless, it is not my role (alone) to police these models. A hoped for side effect of the Web site will be a larger population of educated users with strong intuition into the pros and cons of the models such that the field polices itself. Strictly speaking, these models are appropriate for melting in a 1-D steady state column in chemical equilibrium. How far the real world departs from this model (and how well you can actually tell) is to be decided by data and investigators careful enough to explore the consequences of this model beyond the model itself. It is the gap between model and reality that leads to understanding and better models. I hope that this is just the beginning of that evolution.

## Acknowledgments

[21] Many thanks to Tim Elliott, Rebecca Thomas, Marc Hirschmann, Ken Sims, Matthew Jull, and Ken Rubin for comments on this paper and various versions of UserCalc. Funding for this work is provided by NSF grant OCE96-18706. This is LDEO contribution 6096.

## References

- Allègre, C. J., and M. Condomines, Basalt genesis and mantle structure studied through Th-isotopic geochemistry, *Nature*, 299, 21–24, 1982.
- Elliott, T., T. Plank, A. Zindler, W. White, and B. Bourdon, Element transport from slab to volcanic front at the Mariana arc, *J. Geophys. Res.*, 102, 14,991–15,019, 1997.
- Gill, J. B., and R. W. Williams, Th-isotope and U-series studies of subduction-related volcanic-rocks, *Geochim. Cosmochim. Acta*, 54, 1427–1442, 1990.
- Iwamori, H.,  $^{238}\text{U}$ - $^{230}\text{Th}$ - $^{226}\text{Ra}$  and  $^{235}\text{U}$ - $^{231}\text{Pa}$  disequilibria produced by mantle melting with porous and channel flows, *Earth Planet. Sci. Lett.*, 125, 1–16, 1994.
- Lundstrom, C. C., J. B. Gill, Q. Williams, and M. R. Perfit, Mantle melting and basalt extraction by equilibrium porous flow, *Science*, 270, 1958–1961, 1995.
- McDermott, F., and C. J. Hawkesworth, Th, Pb, and Sr isotope variations in young island-arc volcanics and

- oceanic sediments, *Earth Planet. Sci. Lett.*, *104*, 1–15, 1991.
- McKenzie, D., The extraction of magma from the crust and mantle, *Earth Planet. Sci. Lett.*, *74*, 81–91, 1985.
- Newman, S., J. D. MacDougall, and R. C. Finkel, <sup>230</sup>Th-<sup>238</sup>U disequilibrium in island arcs: Evidence from the Aleutians and the Marianas, *Nature*, *308*, 268–270, 1984.
- Press, W. H., B. P. Flannery, S. A. Teukolsky, and W. T. Vetterling, *Numerical Recipes*, 2nd ed., Cambridge Univ. Press, New York, 1992.
- Qin, Z., Disequilibrium partial melting model and implications for the fractionations of trace elements during mantle melting, *Earth Planet. Sci. Lett.*, *112*, 75–90, 1992.
- Ribe, N. M., The generation and composition of partial melts in the Earth's mantle, *Earth Planet. Sci. Lett.*, *73*, 361–376, 1985.
- Richardson, C. N., and D. McKenzie, Radioactive disequilibria from 2D models of melt generation by plumes and ridges, *Earth Planet. Sci. Lett.*, *128*, 425–437, 1994.
- Sims, K. W. W., D. J. Depaolo, M. T. Murrell, W. S. Baldrige, S. J. Goldstein, and D. A. Clague, Mechanisms of magma generation beneath Hawaii and mid-ocean ridges: Uranium/Thorium and Samarium/Neodymium isotopic evidence, *Science*, *267*, 508–512, 1995.
- Sims, K. W. W., D. J. DePaolo, M. T. Murrell, W. S. Baldrige, S. Goldstein, D. Clague, and M. Jull, Porosity of the melting zone and variations in the solid mantle upwelling rate beneath Hawaii: Inferences from <sup>238</sup>U-<sup>230</sup>Th-<sup>226</sup>Ra and <sup>235</sup>U-<sup>231</sup>Pa disequilibria, *Geochim. Cosmochim. Acta*, *63* (23–24), 4119–4138, 1999.
- Spiegelman, M., and T. Elliott, Consequences of melt transport for U-series disequilibrium in young lavas, *Earth Planet. Sci. Lett.*, *118*, 1–20, 1993.
- Williams, R. W., and J. B. Gill, Effects of partial melting on the <sup>238</sup>U decay series, *Geochim. Cosmochim. Acta*, *53*, 1607–1619, 1989.